Egypt. J. Chem. **Vol. 64,** No. 7 pp. 3913 - 3926 (2021)

Egyptian Journal of Chemistry

http://ejchem.journals.ekb.eg/

Synthesis, Speciation, DNA Binding, Electrochemical and Antiproliferative Properties of Pd(II) Complexes Designed to Improve the Interaction with DNA

Haneen H. AL-Gedany[1], Azza A. Shoukry [2] *, and Saedah R. Al- Mhayawi [3]

[1,3]Chemistry Department, Faculty of Science, University of Jeddah, P.O. Box 80327, Jeddah 21589, Saudi Arabia Jeddah, 21533 Kingdom of Saudi Arabia

[2]Department of Chemistry, Faculty of Science, Cairo University, 12613 Giza, Egypt

Abstract

With the success of cisplatin, further extensive research activities resulted in the discovery of carboplatin (a second-generation drug), where the chloride is replaced by 1,1-cyclobutanedicarboxylate as a new leaving group. In the current study, we continue our previous work on the binding behavior of $[Pd(byp)(H_2O)_2]^{2+}$ with structural features that enhance the interaction with DNA. The coordination properties of 2,2´-bipyridine ligand have been changed such that a versatile ligand can be formed. $[Pd(byp)(gly)]^+$ (1) and [Pd(byp)(CBDCA)] (2), where byp is 2,2´-bipyridine, gly is glycine, and CBDCA is cyclobutane-1,1´-dicarboxylic acid, were synthesized and characterized. The stability constants and stoichiometries of the complexes formed between various DNA unit constituents and $[Pd(byp)(H_2O)_2]^{2+}$ were investigated. The binding properties of the complexes (1) and (2) with CT-DNA were analyzed by UV-vis spectroscopy, viscosity measurements, and cyclic voltammmetry. The determined binding constants for both complexes show strong binding to CT-DNA. The (K_b) values of both complexes are found to be greater than that reported in our previous finding for $[Pd(byp)(H_2O)_2]^{2+}$. The determined (K_b) value for complex (1) (K_b= 4.36x10^3 M^{-1}) as a cationic intercalator, suggests an electrostatic binding mode of the positively charged complex (1) together with hydrogen bonding with the negative sites of the bound DNA. The comparatively higher (K_b) value measured for complex (2) (K_b= 2.11x10^4 M^{-1}) indicates an intercalation mode of binding whereby a ring-opening reaction of CBDCA occurs, followed by the reaction with guanosine 5'-monophosphate to form [(Pdbyp)(CBDCA-O)(5'-GMP)]. The small change in the measured ΔT_m following binding of complex (1) supports strong electrostatic binding, while the significant change in ΔT_m obtained for complex (2) supports the intercalation mode of binding. The two complexes in the absence and in the presence of CT-DNA show quasi-reversible oxidation-reduction redox CV wave . The variation in the values of $E_{1/2}$, ΔEp and I_{pc}/I_{pa} also supports the electrostatic binding of the complex (1) and the intercalation mode for complex (2). The antitumor effects of the two complexes were tested against two different types of cancer cell lines, breast cancer (MCF-7) and colon cancer (HCT-116), as well as one normal cell line; the human normal melanocytes (HFB4). The two complexes display dose-dependent anti-proliferation activity. Complex (2) was shown to have more efficient apoptosis than Complex (1) and may be considered a model for carboplatin with a prediction of improved efficacy against cancer.

Keywords: Pd(II) amine complexes, CT-DNA , Electronic absorption spectroscopy, Cyclic voltammetry, Cytostatic activity, Stability constants.

1. Introduction

Understanding how drug molecules interact with DNA has become an active research area at the interface between chemistry, molecular biology and medicine. Metal-based chemotherapy was first seen at therapeutic level in late 1970s with the application of cisplatin [1]. While cisplatin is still used in form of carboplatin and oxaliplatin, which have less side effects and improved selectivity against certain types of tumors and superior clinical efficacy; it does, however, have adverse side effects such as neurotoxicity, nephrotoxicity, ototoxicity, myelosuppression, vomiting and nausea. Until now, working on developing more efficient medicines is intensified on steric and electronic effects of carrier molecules. In the process of research studies, efforts lead to discovery of carboplatin where the chloride ions are substitution by 1,1-cyclobutanedicarboxylate [2,3]. Carboplatin is less harmful than cisplatin it due to its slower aquation rate but shows comparable behavior when it's used to treat ovarian cancer [4-6].

*Corresponding author e-mail: sazza@sci.cu.edu.eg, azzashoukry@hotmailcom
Receive Date: 30 April 2021, Revise Date: 19 June 2021, Accept Date: 24 June 2021
DOI: 10.21608/EJCHEM.2021.74711.3679

Some researchers regard carboplatin as a prodrug for cisplatin, but others contend that complex $[Pt(NH_3)_2(CBDCA\text{-}O)(5'\text{-}GMP)]$ may be produced through ring opening process when carboplatin interacts with guanosine-5'-monophosphate [6-12]. The formed complex is very stable due to the stacking interaction between CBDCA ring and the suger ring of GMP , which is proofed by the NMR spectra[13]. The displacement of CBDCA by DNA constituent was further studied and proved from the kinetic perspective of the molecular process.[14,15].

In view of the remarkable similarity of coordination chemistry between Pd(II) and Pt(II) complexes, a group of suggestible Pd(II) complexes which mimic the action of similar Pt(II) complexes were utilized as models[16]. In addition, Pd(II) amine complexes also have strong cytotoxicity against certain human tumor cell lines in addition to being able to penetrate sensibly into tumors, bind viably to DNA, and accordingly supress cancer cell replication. Recent progress in research have focused on the molecular basis of the antitumor behavior of palladium(II) with bipyridyl ligands. The molecular structure of various bipyridyl metal complexes whose donors have identical configurations to purine and pyrimidine bases, are considered potent target and strong DNA intercalating agents. [17-22].

Since the effectiveness of Pd(II) drugs is controlled by the carrier ligand (N,N), or (N,O) that actually controls the anticancer property, in this study, the coordinating property of 2,2´- bipyridine ligand has been modified to give a flexible ligand system, formed by addition of glycine or 1,1 CBDCA. We have synthesized and characterized $[Pd(byp)(gly)]^+$**(1)** and [Pd(byp)CBDCA] **(2).** This is expected to have an enhanced effect on the binding ability to DNA, for two reasons, First, the amino group of glycine in complex **(1)** may undergo hydrogen bonding with DNA. Such effects may favor the interaction with DNA, and leads to stronger binding affinity. Second, the stacking interaction between the all the sugar groups of DNA, cyclobutane ring of CBDCA and pyridine ring of 2,2´-bipyridine in complex (**2)** will favor the interaction with DNA. The second effect is like that revealed for carboplatin, from which the stacking interaction between the cyclobutane ring and the deoxyribose sugar of DNA is part of the enhanced cytotoxic antineoplastic activity [23-25].

In this work the formation equilibria of the complexes formed between the diaqua complex (1), $[Pd(byp)(H_2O)_2]^{2+}$ and various DNA sub suits were investigated. The stability constants of the complexes were determined. The concentration distributions of all the different complexes species formed in solution were also evaluated as a function of pH. The DNA binding ability of the two complexes **(1)** and **(2)** with calf-thymus DNA (CT-DNA) was also studied by UV–Vis spectroscopy and several electrochemical techniques. The intrinsic binding constant (k_b) calculated from UV–vis absorption was found to be of higher magnitude than that reported in our previous work on $[Pd(byp)(H_2O)_2]^{2+}$ [24] , which supports improved and enhanced binding abilities of both complexes. The calculated (K_b) values suggest an electrostatic and/or groove binding mode for complex (**1)** and an intercalation binding mode for complex (**2**). This is also supported by the results obtained from thermal denaturation studies, DNA viscosity measurements and cyclic voltammetry**.** The two complexes were screened for their cytostatic activity against two cancer cell lines; the breast cancer (MCF-7) and the colon cancer (HCT-116), as well as one normal cell line; the human normal melanocytes (HFB4). The promising findings of quantitative investigations (both chemical and biological analysis) gained from this study can be correlated to further highlight the significance of this investigation and would hopefully lead to more effective and potent non-platinum based anti-cancer drug candidates.

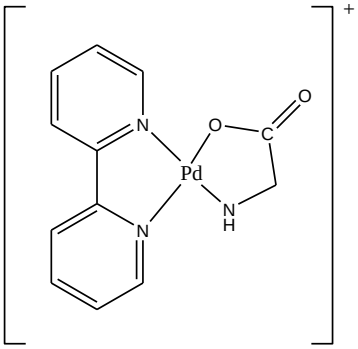

Complex (1)

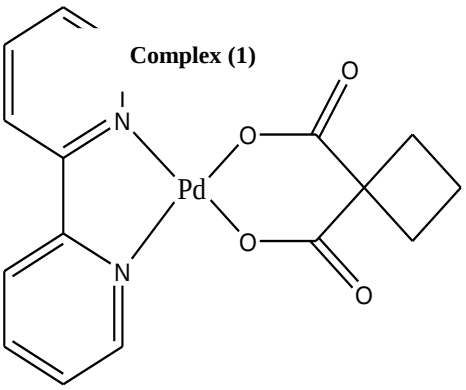

Complex (2)

Experimental

2.1 Materials and reagents

The materials used in this study were of the highest purity presently offered. No further purification of these materials was required. $PdCl_2$, CBDCA, and gly were obtained from Sigma. 2,2´-bipyridine was bought from Sigma Aldrich Chemical Company. The DNA units (thymine, thymidine, adenine, adenosine, guanosine, and guanosine-5' monophosphate) were also given by Aldrich Chem and Acros Organics. The nucleotides were treated with standard HNO_3 solution to be used in the deprotonated form. Calf thymus DNA (CT-DNA) was obtained from Sigma Chemical Co. The chemicals used were of the highest quality. Both DNA-binding experiments were conducted in Tris–HCl buffer solution (50 $mmol.dm^{-3}$ NaCl, 5 $mmol.dm^{-3}$ Tris–HCl, pH 7.1). The Tris-HCl buffer was prepared using deionized, triple distilled water. The solution of CT-DNA in the buffer gave a 2 - 1 ratio of UV-Visible absorption at 260 and 280 nm, [18], meaning that the DNA was sufficiently free of protein. The concentration of DNA was measured by spectrophotometry (ε = 6,600 $mol.dm^{-3}.cm^{-1}$) [26]. The stock solution of DNA was kept at -20 °C. The chemicals were prepared by dissolving them in deionized water shortly before application.

2.2 Synthesis of the complexes

$[Pd(byp)Cl_2]$ was produced by heating $PdCl_2$ (200.0 mg, 1.129 mmol) in 40 ml H_2O and KCl (168.2 mg, 2.256 mmol) to 70ºC for thirty minutes. The completely clear solution of $[PdCl_4]^{2-}$ was cooled to 25ºC, filtered and then the ligand 2,2´-bipyridine (176.327 mg, 1.129 mmol), dissolved in 10 ml H_2O was dropwise added to the solution with continuous stirring. The pH was kept at 2–3 by adding HCl NaOH. A brownish-yellow precipitate of $[Pd(byp)Cl_2]$ was formed and stirred for the more 2 hours at 50ºC. The precipitate was filtered and carefully washed by treating with purified water, ethanol, and diethyl ether for three times. A yield of brownish-yellow powder was obtained. Anal. for the $[Pd(byp)Cl_2]$, $C_{10}H_8N_2PdCl_2$: Calc. (%): C, 36.0; H, 2.40; N, 8.40. Found: C, 35.78; H, 2.02; N,8.2%.

Conversion of $[Pd(byp)Cl_2]$ into the diaqua forms was performed by treatment with two equivalents of $AgNO_3$ as mentioned before [17,22]. The following general method was carried out for the synthesis of the ternary complexes (1) and (2). The $[Pd(byp)Cl_2]$ (333.5 mg, 1 mmol) was added to (337.5 mg,1.98 mmol) $AgNO_3$ in 10 ml H_2O at 25°C, the mixture was stirred in the dark for 24 hours. After filtering off the white precipitate (AgCl), the filtrate was applied to; (75.07 mg, 1 mmol) for glycine and (144.1 mg, 1 mmol) for H_2CBDCA, respectively. The pH value was balanced between 4.0-5.0 with NaOH, and the solution was stirred for another 2 hours at 60°C and kept at 4°C overnight. The precipitated complexes were isolated by vacuum filtration washed three times with H_2O, ethanol and diethyl ether. Elemental carbon, hydrogen, and nitrogen analyses were performed with a Perkin- Elmer 240 elemental analyzer. For the $[Pd(byp)(gly)]^+.H_2O$, $PdC_{12}H_{15}O_3N_3$ Calculated (%): C, 40.51; H, 4.22; N, 11.81. Found (%): C, 40.67; H, 4.18; N, 12.11 and for $[Pd(byp)(CBDCA)].H_2O$, $PdC_{16}H_{16}O_5N_2$ Calculated (%): C, 45.66; H, 3.78; N, 6.62. Found (%): C, 45.45; H, 3.72; N, 6.72.

2.3 Antitumor activity

Antitumor activity in vitro was evaluated by using a system based on the tetrazolium salt (MTT). The antitumor activity was tested on two cancer cell lines; the breast cancer (MCF-7) and colon cancer cell line (HCT-116) , as well as one normal cell line; the human normal melanocytes (HFB4). Cells were cultured at 37ºC under a humidified atmosphere of 5% CO_2 in RPMI 1640 medium supplemented with 10% fetal serum and dispersed in replicate 96- well plates with 1 $\times 10^4$ cells per well before treatment with the complexes. Various concentrations of the tested complexes (0, 50, 100, 150, 200 and 250 μM) were incubated to the cells with the studied complexes. Monolayer triplicate wells were utilized for each individual dose. After 72 h exposure to the toxins, cell viability was determined by measuring the absorbance at 570 nm with an enzyme-linked immunosorbent assay (ELISA) reader. Each test was performed in triplicate. The relation between surviving fraction and complex concentration is plotted to get the survival curve of each tumor cell line after the specified complex. The IC_{50} values where derived from the experimental data to provide an estimate of the drug concentration required to block 50 percent of the desired action. Assays were performed at the National Cancer Institute in Cairo University, Egypt.

2.4 Apparatus and procedure

On a Metrohm 686 titroprocessor, titrimetrical measurements were performed with a 665 Dosimat. Pure buffer solutions were used to calibrate the electrodes[27]. The measurements were conducted in an atmosphere of nitrogen at 25°C. Using the TB-85-shimadzu UV spectrophotometer, spectrophotometric experiments were carried out. Determination of the acid dissociation constants of the studied DNA units were performed by potentiometric titration of sample of 0.05 mmol. dm^{-3} against standard NaOH solutions (0.05 $mmol.L^{-1}$), as well as for the that of coordinated water in $[Pd(byp)(H_2O)_2]^{2+}$. Solution mixtures containing

$[Pd(byp)(H_2O)_2]^{2+}$ (0.05 mmol.dm^{-3}) and (0.10 mmol) ligand were used to determine the formation constant of complexes in a concentration ratio of 1:2 (Pdcomplex :DNA ligand). Each solution mixture had a volume of 40 ml , the ionic strength was kept constant at 0.1 mol.dm^{-3}. The pH measurements were converted to a concentration of hydrogen ions. [16]. The formed species are characterized by the overall general balanced equilibrium.

$$pM + qL + rH \rightleftharpoons (M)_p(L)_q(H)_r \qquad (1)$$

The formation constants are specified by

$$\beta_{pqr} = \frac{[(M)_p(L)_q(H)_r]}{[M]^p[L]^q[H]^r} \qquad \textbf{(2)}$$

where M, L, and H stand for $[Pd(bpy)(H_2O)_2]^{2+}$ ion, ligand, and protons respectively. The calculations were done using the computer software MINIQUAD-75. Composition models were developed to establish the stability constants and the stoichiometry of the formed complexes. The best mathematical fit model for the data was selected, as mentioned previously[28]. The graphs showing the concentration distributions were obtained from data applying the well known program SPECIES [29] under the prescribed experimental conditions.

2.5 DNA Binding Studies

2.5.1. Electronic absorption spectroscopy

The use of UV-Vis spectroscopy is popular in order to identify transition between energy levels in a molecule and to gain information on configurations and structure of a species. All experiments were performed on a Shimadzu UV-1800 spectrophotometer having a simulator and cell temperature controller . The UV spectrophotometer has been used to analyze the interaction of 20 µmol.dm^{-3} of complexes (1) and (2) with differing DNA concentrations in the range of 0 to 160 µmol.dm^{-3}. To eliminate the absorbance value of free CT-DNA, equal quantities of DNA were applied to both the palladium complex and the reference solution. Tris buffer has been used as the consensus reference solution. Absorption values were reported during each addition of CT-DNA solution, after its subsequent equilibration (ca. 10 min). All the sample were scanned in the range of 200–400 nanometers. Each sample was analysed more than one time and an average value was calculated. The obtained Uv-Vis spectral data were analyzed in order to evaluate the intrinsic binding constants K_b of the complexes (1) and (2) with CT-DNA.

Thermal denaturation tests were performed at 260nm to determine the melting temperature (Tm) of DNA. Tm is well defined as the temperature where 50 percent of the double stranded DNA is transformed to single stranded DNA . Tm was calculated for the free CT-DNA in Tris–HCl buffer pH 7.1, both in the absence and presence of the complexes at a concentration of 60 µM CT-DNA and 20 µM complex . Samples were heated and continuously stirred under increasing temperature from 25 to 95 °C, taking an absorbance reading after each 5 °C increment. The denaturation temperature (Tm) was taken as the midpoint of the hyperchromic transformation and as the average value for three measurements of (Tm).

2.5.2. Viscosity measurements

Stabinger Viscometer TM SVM 3000 was used to perform viscosity titration studies through varying the concentration of the two complexes (1) and (2) at (20, 40, 60, 80, 100) µM with (100 µM) CT-DNA concentration. The flow time of the samples was carefully measured several times and an average value of all measurements were taken at the end . The data is plotted as the binding ratio ([complex]/[DNA]) versus $(\eta/\eta^0)^{1/3}$, in which η^0 was the viscosity value of free CT-DNA and η was the viscosity value for DNA in presence of either **(1)** and **(2)** [30].

2.5.3. Cyclic voltammetry measurements

The cyclic voltammetry measurements were made using 797 VA computrace. The electrochemical measurements were calculated in a 10 ml electrolytic cell in 50 mM NaCl buffer with pH 7.0. The voltammogram was recorded for 10 ml of solution containing 100-µM complexes (1) and (2), and free DNA. To assess the results of differing DNA concentrations, 10 ml samples were prepared at constant concentrations of 100 µM complexes , with varying DNA concentrations. For complex (1), the molar concentrations were (20, 60, and 160 µM) in the molar ratio of (1:0.2, 1:0.6 and 1:1.60) respectively. For complex (2) the concentration of DNA used were (DNA = 20, 60, 80, 120 and 160 µM); in the molar ratio . (1:0.2, 1:0.6, 1:0.8, 1: 1.25 and 1:1.60).

3. Results and Discussion

3.1 Complex formation equilibria

The pKa values of the DNA constituent were determined under the same conditions used to determine the pKa values of ternary complexes formed with Pd(II). The determined ligand dissociation constants were found to be consistent literature data. [21-28]. (Actual Notes). The analysis

of the potentiometric titration data of $[Pd(byp)(H_2O)_2]^{2+}$ was in agreement with the previously investigated data [32], revealing the formation of the species 10 –1, 10-2 and 20-2. Fig.1 depicts the distribution diagram for $[Pd(byp)(H_2O)_2]^{2+}$and its hydrolyzed species . At pH 4, the dimer with a single hydroxo bridge reaches a maximum concentration of 20%, whereas the monohydroxo species (10-1) grows in concentration with increasing pH, reaching a maximum concentration of 78% at pH 4-8. This reveals that, the dominant species at the physiological pH range, is the mono hydroxo species 10-1.

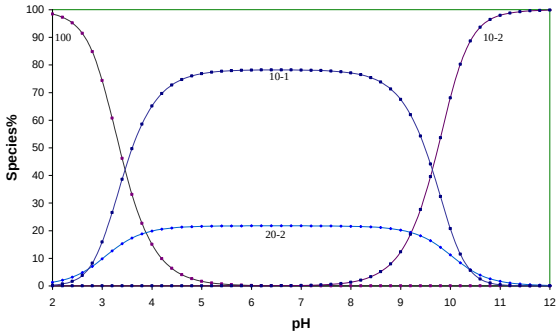

Fig. 1. Concentration distribution of various species as a function of pH for hydrolysis of 1.25 mmol.L^{-1} $[Pd(byp)(H_2O)_2]^{2+}$

The data obtained for the pH titration of $[Pd(bip)(H_2O)_2]^{2+}$ with the examined DNA subunits show the formation of of 1:1 and 1:2 complexes. The monodentate pyrimidines: thymine and thymidines , contain only basic nitrogen donor atoms at (N_3-C_4O group) in the measurable pH range, which allows the formation of a 1:1 and 1:2 complexes with the $Pd(byp)^{2+}$ complex ion (Table 1). The complexes of the pyrimidines are formed above pH 4 due to the relatively high pH values of the pyrimidines (pKa≈8) which ascertain the importance of binding sites of the pyrimidines at the neutral and the weakly basic pH range. In addition to 1:1 and 1:2 complexes, (5′-GMP), adenine and adenosine also form the protonated complexes which could be detected at comparatively lower pH range. It is indicated that binding at the sites are pH dependent. The pK_a of N1H of guanosine is 9.12, and that of N7H is 1.2**.[29].** It was reported [33] that, in the acidic the metal ion coordinates to N7 and N1 remained protonated. The pK_a of the protonated complexes of $Pd(byp)^{2+}$ with guanosine is 4.10, which implies that N1H remains protonated at lower pH its acidity increase by by 5.02 unit (9.12-4.10) . At higher pH the binding site were disputed and binding sites are suggested to change from N7 to N1 [21]. (5′-GMP) forms a stronger complex with $[Pd(byp)(H_2O)_2]^{2+}$ than guanosine; $\log\beta_{110}$ 11.55 compared to 9.30 for guanosine. The increased stabilization results from the negatively charged 5′-GMP^{3-} ion. 5′-**G**MP forms mono- and diprotonated complexes. The pK_a values of the protonated species corresponding to -PO2(OH) group is 3.43 ($\log\beta_{112}$-$\log\beta_{111}$) whereas, that corresponding to N1H group is 4.01 ($\log\beta_{111}$- $\log\beta_{110}$). Worth mentioned here that the N_1H groups were acidified upon complex formation by 5.24 (9.28-4.04) pK_a units, which is consistence with pervious work [16] reported on GMP complexes. No significant acidification was observed on the phosphate group upon complex formation, since it is located relatively far from the coordination center. Fig 2 shows the distribution diagram of all the species formed in the (Pd(byp)-5'-GMP system). From the figure it is clear that the deprotonated species 112 exists at low pH up to pH 3.5 . At slightly higher pH the phosphate –O will start to be involved in coordination and accordingly the 111 species will appear. The species 110 is formed and previels at a higher pH (4-6) ; the most probable site, through coordination of N7AO6 site. The 120 species prevails at a pH higher than 7.8 and reaches a maximum (100%) at pH 9.3. Previous research has proposed that N9 is the coordination position of adenine in the palladium(II) complex [29,30]. Table 1 shows the presence of the protonated species 111 and 121 which confirms the change of coordination sites upon varying the pH. At low pH, the N9H is still protonated, as is further confirmed by the higher pK_a value, (9.40) for the 121 species and acidification of the N9H in the species 111 by 4.48 (9.29-4.81). Upon increasing pH, N9 H becomes deprotonated and the binding site shifts to N9

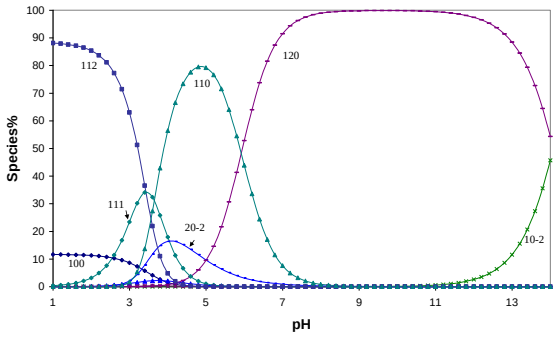

Fig.2. Concentration distribution of various species as a function of pH for the Pd(byp)–guanosine-5'-monophosphate system (1.25 mmol.L^{-1} of $Pd(byp)^{2+}$ and 2.5 mmol.L^{-1} for guanosine-5'-monophosphate)**.**

Table(1) Formation constants for complexes of $[Pd(byp)(H_2O)_2]^{2+}$ with DNA-Unit constituents at 25 ºC and 0.1M ionic strength.

System	M	L	H[a]	log β[b]	pK^c_a	S[c]
Thymine	0	1	1	9.58(0.00)	9.58	8.7E-8
	1	1	0	8.44(0.32)		6.3E-8
	1	2	0	14.16(0.13)		
Thymidine	0	1	1	9.50(0.00)	9.50	8.1E-8
	1	1	0	8.30(0.04)		4.1E-8
	1	2	0	14.09(0.08)		
Guanosine	0	1	1	9.12(0.01)	9.12	6.7E-8
	1	1	0	9.30(0.08)		2.1E-7
	1	1	1	13.40(0.03)	4.10	
	1	2	0	14.00(0.01)		
.	1	2	1	19.86(0.04)	5.86	
Guanosine 5'-monophosphate	0	1	1	9.28(0.01)	9.28	6.6E-8
	0	1	2	15.41(0.01)	6.13	9.7E-7
	1	1	0	11.55(0.19)		
	1	1	1	15.59(0.74)	4.04	
	1	1	2	19.02(0.45)	3.43	
	1	2	0	20.69(0.64)		
	1	2	1	26.61(0.47	5.92	
Adenine	0	1	1	9.29(0.01)	9.29	9.4E-8
	0	1	2	13.32(0.02)	4.03	
	1	1	0	10.72(0.40)		4.7E-8
	1	1	1	15.53(0.31)	4.81	
	1	2	0	15.36(0.16)		
	1	2	1	24.76(0.20)	9.40	
Adenosine	0	1	1	3.60(0.01)	3.60	
	1	1	0	6.99(0.04)		3.26E-8
	1	1	1	10.22(0.05)	3.23	
	1	2	0	14.31(0.03)		
	1	2	1	17.78(0.07)	3.47	

M, *L* and H^a are the stoichiometric coefficients corresponding to Pd(byp), DNA units and H^+ respectively; [b] Standard deviation are given in parentheses; [c]Sum of square of residuals.

3.3. Antitumor activity

The cytotoxic effect of complexes may be due to induced oxidative stress which results in cell death by triggering apoptotic processes or necrosis. In this study, cytotoxic impact of different concentrations of the two synthesized Pd(II) complexes (1) and (2) in the range of (0, 50, 100, 150, 200 and 250 μM) are being screened successfully against human invasive breast cancer cell line (MCF-7) human colon carcinoma (HCT-116) as well as on normal human melanocyte (HFB4). The cells were exposed to each compound for a span of 48 hours so that the complexes would

enter the DNA or some other biological target. TheIC_{50} value of the complexes , which indicates the concentration required to make 50% of inhibition in vitro in the lab was detected from the experimental datas. The results are presented in Figure 3 (a) and 3 (b). The production of MCF-7 and HCT-116 was strongly decreased upon increasing the concentration of complexes. Complex **(1)** Fig. 3 (a) shows IC_{50} value equals 78.1 μM with MCF-7 and 81.9μ M for HCT-116. Data are presented in Table II. Fig. 2(b) shows that the cytotoxicity of complex (**2)** against the same tested cancer cells lines is much higher than that observed for complex (**1)**, as shown by the much stronger decrease of the proliferation of MCF-7 and HCT-116 on increasing the complex concentration, with the IC_{50} value equals 66.9μM with MCF-7 and 68.1 μM with HCT-116. Complex (2) shows lower $IC_{50.}$ (Table III) which reveals its higher tumor inhibitory activity.

It is well reported that the antitumor activity of carboplatin is believed to be caused by the ring opening of the coordinated CBDCA and interaction with DNA [12]. The formed adduct is stabilized by stacking interaction between the sugar group of the DNA and cyclobutane group of CBDCA. In the present study, [Pd(byp)(CBDCA)] will interact with DNA through the ring opening of coordinated CBDCA and creating new stable adduct, stabilized by stacking interactions

between the sugar group of DNA and the cyclobutane ring of coordinated CBDCA as in the case of carboplatin . Moreover, additional stabilization is provided by the π-stacking interaction with the two bipyridine rings. These structural features make [Pd(byp)(CBDCA)] an effective model for carboplatin with promising cytostatic activity.

Noteworthy about these results is that each of the complexes caused a slight effect on human normal cells, unlike most other anticancer agents that affect both healthy and cancerous cells. Therefore, it is claimed that both complexes (1) and (2) could be applied as a specific target for cancer cell DNA

a

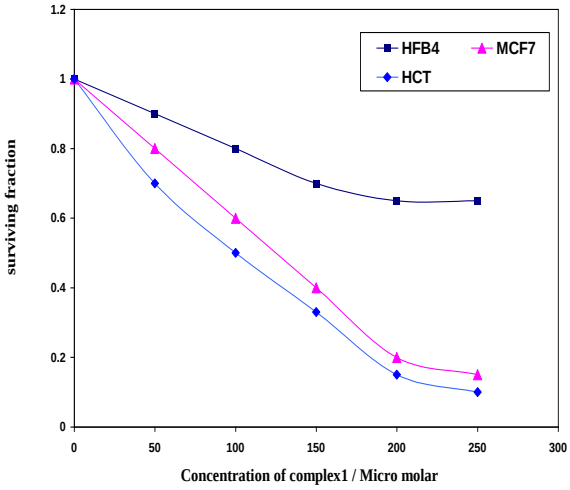

b

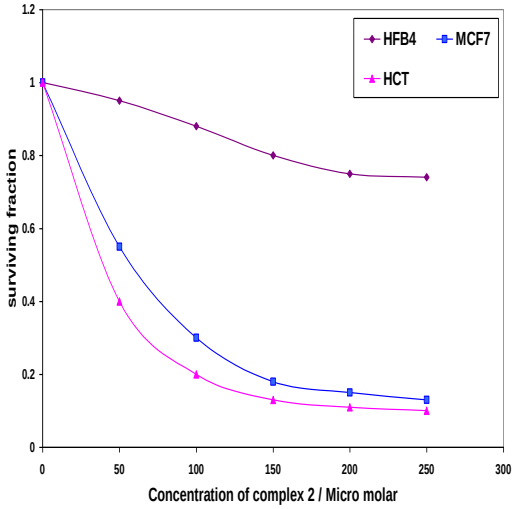

Fig. 3. Relationship between the concentration of complexes **1 (a)& 2(b)** and the surviving fraction of HCT-116 (human colon cancer cell line), MCF-7 (human breast cancer cell line) and HFB4 (human normal melanocytes)

Table II. IC_{50} values of $[Pd(byp)(H_2O)_2]^{2+}$determined after 48, 72, h incubation. Each test was performed in triplicate

	48 hr		72 hr	
Cell line	IC_{50}(μM)	r^2	IC_{50}(μM)	r^2
(HCT-116)	98.5	0.99	81.9	0.96
(MCF-7)	121.2	0.96	78.1	0.97
HFB4	> 150	0.96	> 100	0.95

Table III. IC_{50} values of [Pd(byp)(CBDCA)]determined after 48 and 72 h incubation. Each test was performed in triplicate

	48 hr		72 hr	
Cell line	$IC_{50}(\mu M)$	r^2	$IC_{50}(\mu M)$	r^2
HCT-116	68.1	0.97	48.5	0.97
MCF-7	66.9	0.93	66.7	0.93
HFB4	> 250	0.97	> 250	0.97

3.4. DNA Binding Studies

3.4. 1. Electronic absorption spectroscopy

Transition metal complexes can bind to DNA via both covalent and/or non covalent interactions. UV spectroscopy was used to examine the interaction of the two complexes (1) and (2) with CT-DNA and to explore the potential binding modes and to calculate the inherent binding constants (K_b). We preserve a constant concentration of the complexes ([complex] = 20 μ M) and vary the concentration of CT-DNA upon measuring the spectrum of the two complexes. The Pd(II) complexes showed maximal absorption at wavelength of λ_{max} = 216 nm for (1) and λ_{max} =314 nm for (2), as seen in Figs.4 and 5 respectively. This displacement is due to the π–π* transition of the coordinated ligands. A continuous increase in absorption (hyperchromism) was observed upon titrating the two complexes by CT-DNA. This red shift suggests that the direct association with CT-DNA results in the formation of a new complex with double helical CT-DNA being more stabilized. Complex (1) showed an observed continuous red shift up to a wavelength of λ_{max}= 252. Whereas, complex (2) displayed an increase in absorption intensity at λ_{max} =303 and λ_{max} = 314 (both were at maximum absorbance). A complete characterization of DNA binding agents require that their mode of binding to DNA be established. In order to monitor and compare the magnitude of the binding strength of complexes to CT-DNA, the intrinsic binding constants K_b is measured. It represents the binding constant per DNA base pair. It can be calculated by following the change in absorbance st λmax, with increasing concentration of CT-DNA,according to the following equation [34].

$$\frac{[DNA]}{(\varepsilon_a - \varepsilon_f)} = \frac{[DNA]}{(\varepsilon_b - \varepsilon_f)} + \frac{1}{K_b(\varepsilon_b - \varepsilon_f)} \qquad (3)$$

where [DNA] is the base pair concentration of DNA, ε_f, ε_a, and ε_b are the extinction coefficients for free Pd (II) complexes, for each addition of DNA to the Pd (II) complex, and the complex in completely bound form respectively. (K_b) was obtained by plotting [DNA]/($\varepsilon_a - \varepsilon_f$) versus [DNA] , inset of the plots in figures3 and 4, and given by the ratio of slope to the intercept. The intrinsic binding constant (K_b) for complex (1) was 4.36 x 10^3 M^{-1} (R^2 = 0.974 for seven points) and for complex (2) (K_b) was 2.1 104 M^{-1} (R^2 = 0.965 for seven points). The calculated (K_b) values for both complexes (1) and (2) reveal a strong binding to CT-DNA.

Is it important to notice that the calculated (K_b) value of complex (1) is higher than that previously reported in our previous work on the diaqua complex $[Pd(byp)(H_2O)_2]^{2+}$. This is due to the fact that the DNA double helix has many accessible hydrogen bonding sites, both in the minor and major groove , and it is likely that the amino group in glycine in complex (1) form hydrogen bonds with DNA. This would result in a comparatively higher DNA binding strength than that reported for diaqua $[Pd(byp)(H_2O)_2]^{2+}$[24]. The higher (K_b) value obtained for complex (2); ($K_b = 2.1\times10^4\ M^{-1}$) could be attributed to CBDCA ring opening, coordination to DNA, and formation of very stable adduct which is stabilized by π-stacking interaction as previously reported for carboplatin.

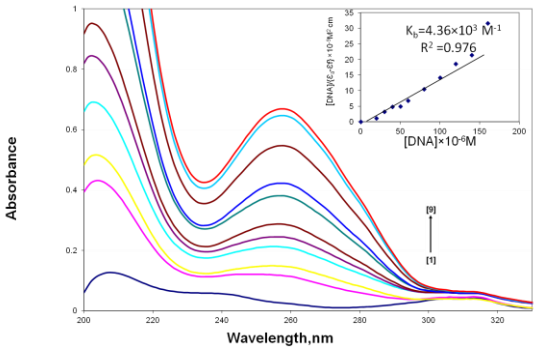

Fig. 4. Absorption spectra of [Pd(byp)(gly](1) in Tris–HCl buffer upon addition of CT-DNA. [complex] = 20 µM, [DNA] = (0) [1], (40) [2],(50) [3],(60)[4],(80)[5],(100) [6], (120) [7],(140) [8], (160) [9] µM. Arrow shows the absorbance changing upon the increase of DNA concentration. Inst: Plot of [DNA]/(ε_a–ε_f) versus [DNA] for the titration of CT-DNA with the complex.

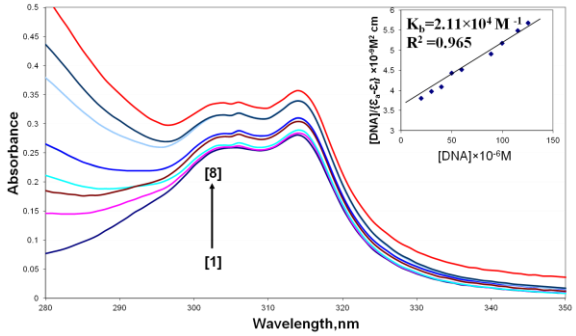

Fig. 5 Absorption spectra of [Pd(byp)(CBDCA)](2) in Tris–HCl buffer upon addition of CT-DNA. [complex] = 20 µM, [DNA] = (0) [1], (20) [2],(40) [3],(60)[4],(80)[5],(100) [6], (120) [7],(160) [8] µM. Arrow shows the absorbance changing upon the increase of DNA concentration. Inst: Plot of [DNA]/(ε_a–ε_f) versus [DNA] for the titration of CT-DNA with the complex

3.4.2. Thermal denaturation

Metal complexes are known to be capable of transforming supercoiled DNA into open circular DNA. The interaction strength of complexes and their binding abilities to DNA could be studied by following the thermal behavior of DNA in absence and presence of complexes It can be analyzed very precisely using UV/Vis spectroscopy The double-stranded DNA tends to gradually dissociate to single strands upon increasing solution temperature and generates a hyperchromic effect on the absorption spectra of DNA bases (λ_{max} = 260 nm). The melting of DNA can be monitored very efficiently using UV/Vis absorption spectroscopy. When DNA melts and the two strands separate, the electronic interaction ns between the bases are modified and the entire absorption spectrum increases in intensity [37]. Previous studies have revealed that when a cationic species interact with double helix the stability increases and so does the DNA melting temperature [39]. The binding of a ligand to a nucleic acid induces its conformational change to increase the denaturation temperatures ,depending on the strength and mode of its interaction with the nucleic acid. In general, groove binding or electrostatic binding along the phosphate backbone of DNA gives rise to only a small change in thermal denaturation temperature, while intercalation binding mode leads to a significant rise in thermal denaturation temperature of DNA due to the stabilization of the Watson–Crick base paired duplex [39,40]. The DNA melting studies for the present complexes show a positive shift in the melting temperature (ΔT_m) of nearly 5°C for complex **(1)** and ≈11 °C for complex **(2)** as shown in Figure 6. Here $\Delta T_m = T_m - T^0_m$, where, T_m and T^0_m refer to the melting temperature of DNA in presence and absence of complexes respectively. This indicates primarily electrostatic and/or groove binding nature of complexes **(1)** in preference to an intercalative mode of binding to DNA [41] which is in accordance with the results of the absorption titration experiments and the calculation of (K_b). The relatively higher ΔT_m value observed for complex **(2)** suggest an intercalation mode of binding and stronger binding strength to CT-DNA, Intercalation of the complexes between DNA base pairs causes stabilization of base pair stacking and hence raises the melting temperature of double-stranded much more than electrostatic binding mode. This could be attributed to ring opening of CBDCA ring and stabilization of base pair which is in accordance with the observed higher K_b value for the same complex.

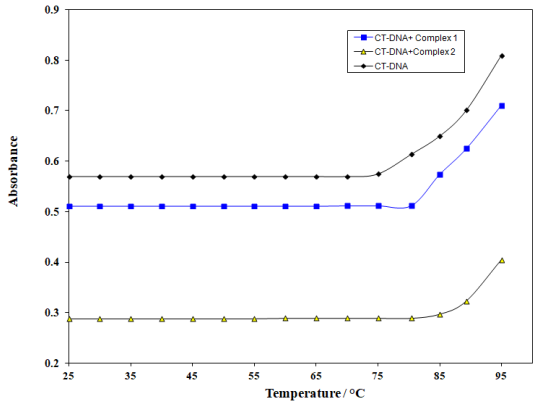

Fig. 6. Melting curves of CT-DNA in Tris–HCl buffer in absence and presence of complexes, [DNA] = 60 µM, [complex] = 20 µM

3.4.3. Viscosity measurements

The nature of binding characteristic of complexes **(1)** and **(2)** were further investigated by viscosity measurements on the CT-DNA solution incubated with an increasing concentration of the complexes. Although optical photophysical probes usually offer essential information about the binding modes of complexes to DNA, they lacke some evidences supporting the intercalative binding model [40]. The measurements of CT-DNA viscosity are regarded as the least ambiguous and the most critical tests of a binding model in solution in the absence of crystallographic structural data. A plot of relative specific viscosity $(\eta/\eta_0)^{1/3}$ versus [complex]/[DNA], where η and η_0 are the specific viscosity contribution of DNA in the absence and presence of the complexes is shown in Figure 7. Cisplatin is well known to kink DNA through covalent binding, shortening the axial length of the double helix [43] and caused a decrease in the relative viscosity of the solution. Whereas the classical organic intercalators such as ethidium bromide increases the axial length of the DNA and makes it more rigid [44,45] based on the classical intercalation model which demands that the DNA helix lengthens as base pairs are separated to accommodate the bound ligand, resulting in an increase in the relative viscosity. As can be seen from Fig. 6, a significant increase in the relative specific viscosity of DNA solution was observed with increasing concentration of both complexes **(1)** and **(2)**. Thus we may deduce that the complexes, certainly, are DNA intercalator. From Figure 6, it is also clear that the greater increase in DNA viscosity up on / addition of complex **(2)** is relatively higher than that obtained upon addition of complex (1). This also supports the stronger binding ability of complex (2) relative to that of complex (1) which is in agreement with spectrophotometric data.

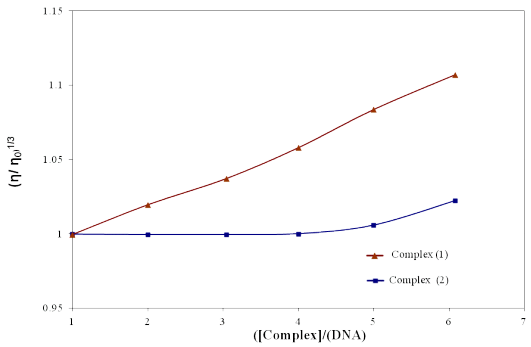

Fig. 7. The effect of increasing amount of complexes (1) and (2) on the relative viscosity of CT-DNA at 25± 0.1ºC, ([DNA] = 20, 40, 60, 80, 100µM).

3.4.4. Cyclic voltammetry measurements

When nucleic acids are placed in contact with electrodes, they are usually strongly adsorbed and undergo charge-transfer reactions producing signals that can provide information about their type, concentration, changes in structure, and their interaction with various compounds. The *in vitro* redox behavior of electrochemically active molecules in the absence and presence of DNA can be used to analyze their DNA binding potentials [46,47] as well as in probing the nature and mechanism of binding to DNA [46]. The technique was utilized in the current study with this prospective, and to provide a useful complement to the above method of investigation. The redox behavior of the two complexes **(1)** and **(2)** in absence and presence of CT-DNA was studied at room temperature within potential range of -1400 to 0.00 mV for complex **(1)** and -1200 to 0.00 mV for complex **(2)**, at a scan rate of 200 mVs^{-1}. The results indicate that, the two complexes are redox active and show quasi-reversible cyclic voltammetric response. The cyclic voltammogram of complex **(1)** exhibits a quasi-reversible redox wave with E_{pc} and E_{pa} values of -424 and -654 mV, respectively. The ratio of cathodic to anodic peak currents I_{pc}/I_{pa} was 0.15. The formal electrode potentials $E_{1/2}$, ΔE_p (difference in cathodic E_{pc} and anodic E_{pa} peak potentials) were -539 and 230 mV respectively. At constant temperature, the addition of CT-DNA resulted in the shift in $E_{1/2}$ = -559 mV and ΔE_p = 224 mV, Fig.8. The ratio of I_{pc}/I_{pa} is 0.10 for CT-DNA bound metal complex. On plotting the cyclic voltammogram of complex **(2)** in a scan rate of 200 mVs^{-1} it is noted that the redox wave is quasi-reversible with $E_{1/2}$, ΔE_p and I_{pc}/I_{pa} values of -685.5 mV, 143 mV and 0.36 respectively. Upon addition of CT-DNA under the same recording conditions complex **(2)** experience a shift in $E_{1/2}$ (-628 mV), ΔE_p (135 mV) and ratio of anodic to cathodic peak currents I_{pc}/I_{pa} is 0.11, Fig.9. The observed shift in potentials and decrease in current ratio suggest the binding of both complexes **(1)** and (2) to CT-DNA [48,49].

The variation in the formal potential can be used to decide how a drug can interact with DNA interaction. In general, it was reported that the positive shift (anodic shift) in formal potential is caused by the intercalation of the cationic drug into the double helical structure of DNA, while negative shift is observed for the electrostatic interaction of the cationic drug with the anionic phosphate of DNA backbone [50,51]. The obvious negative peak potential shift (cathodic shift) in the CV behavior of complex **(1)** by the addition of DNA suggests an electrostatic interaction of complex **(1)** with the

polyanionic DNA, as was reported previously for the diaqua complex $[Pd(byp)OH_2)]^{2+}$ [18], but with much stronger binding affinity, due to hydrogen bonding of glycine to the electronegative sites of DNA. Wherase, the positive shift in formal potential of complex **(2)** (i.e from $E_{1/2}$ (-685 mV) to $E_{1/2}$ (-628 mV)) supports our previous inference for intercalation binding mode of complex **(2),** where the cyclobutane ring undergo stacking interaction with the sugar group of the bound DNA as previously proposed and form hydrophobic contact with the purine rings of IMP and GMP. Such hydrophobic contacts may contribute to the stabilization of the quaternary complexes. The same finding was obtained from an NMR investigation of the carboplatin–GMP complex [6]. This is in agreement with the data obtained from the studied analytical and spectroscopic techniques, and further supported the findings of biological analysis.

The effect of concentration of CT-DNA on potential and current peaks of the complexes (**1)** and (**2)** was also studied using a constant concentration of the complex (100 µM) and varying the concentra-tion of CT-DNA (20, 60, and 160µ M) of complex (1) and (20, 60, ,80,120 and 160µ M) of complex (2). (Fig. 10 (a) and (b). The results showed that the incremental addition of CT-DNA to both complexes causes a diminution of the peak currents due to variation of the binding state and slowing the mass transfer of the complex after binding to CT-DNA fragments as well as a shift in the $E_{1/2}$. The decrease of the anodic and cathodic peak currents of the complexes in presence of DNA is due to formation of slowly diffusing complex-DNA supramolecular complex, which in turn lowers the concentration of the free complex (mainly responsible for the transfer of current.

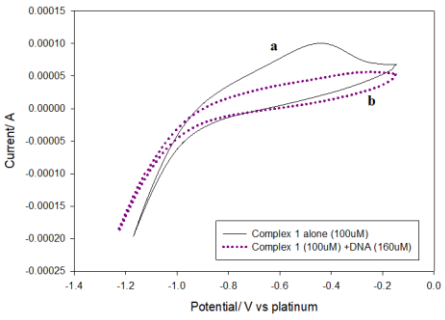

Fig. 8. Cyclic voltammograms of complex (1) in absence (a) and presence (b) of CT- DNA. ν = 200 mV s^{-1}, [complex] = 100 µM; [DNA]: (a) 0, (b) 160 µM

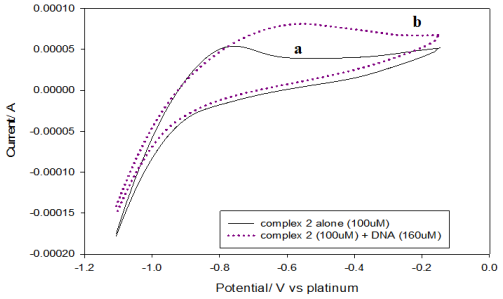

Fig. 9.: Cyclic voltammograms of complex (2) in absence (a)and presence (b) of CT-DNA. ν = 200 mV s^{-1}, [complex] = 100 µM; [DNA]: (a) 0, (b)160 µM

(A)

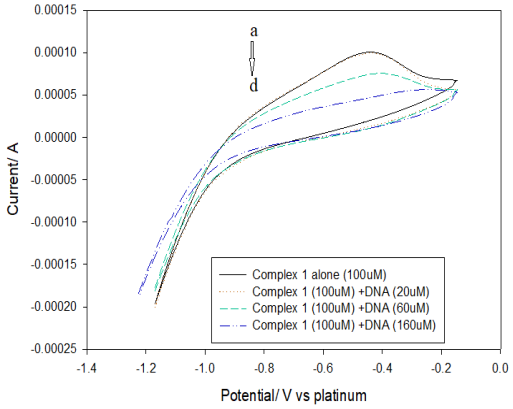

(B)

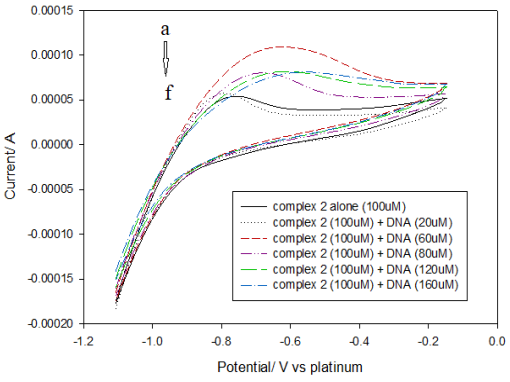

Fig.10. (A). Cyclic voltammograms of 100 µM of complex (1) (A) in absence (a) and presence of different concentrations of DNA. 20 µM DNA (b), 60 µM DNA (c) and 160 µM DNA (d). m = 200 mV s^{-1}. (B) Cyclic voltammograms of 100 µM of complex (2)) HCl buffer in the absence (a) and presence of 20 µM DNA (b), 60 µM DNA (c) 80 µM DNA (d) 120 µM DNA (e) and 160 µM DNA (f). m = 200 mV s^{-1}

Conclusion

Metal-based anti-cancer agents are more effective and selective for chemotherapy as compared to other anti-cancer therapeutics currently available in the market. The therapeutic and pharmacological efficiencies and structures of compounds can often be modified to enhance the coordination of DNA with metal ions and results in significance hindered or suppressed function of the nucleic acid in physiological processes. The present investigation is a continuation of our previous work on complex formation equlibria and DNA binding studies of $[Pd(byp)(H_2O)_2]^{2+}$ with CT-DNA[24]. The equilibria of the complexes formed between $[Pd(byp)(H_2O)_2]^{2+}$ with some selected DNA constituents was investigated. The results of equilibrium studies reveal the formation of mixed-ligand complexes in the physiological pH range, which reflects the biological significance of these complexes for pharmaceutical and biomedical research.

In a search for a new model of carboplatin, in this study the coordinating property of 2,2´ bipyridine ligand has been modified to give a flexible ligand system, formed by addition of glycine or 1,1-CBDCA to enhance the binding ability to DNA. We have synthesized and characterized $[Pd(byp)(gly)]^+$ **(1)** and [Pd(byp)CBDCA] **(2)**. The amino group in glycine may stabilize the DNA adduct with Pd(II) complexes, through bonding with the negatively charged phosphate backbone at the periphery of the double helix CT-DNA. Also bipyridine ring in addition to cyclobutane ring may undergo stacking interaction with the sugar group of the bound DNA as previously reported [6]. It is interesting to note that the calculated binding constant for both complexes was found to be higher than that reported for $[Pd(byp)(H_2O)_2]^{2+}$ [24] indicating stronger binding ability of both complexes. The results from UV-Vis spectroscopy, as well as thermal denaturation, viscosity, and cyclic voltammetry data, all reveal electrostatic binding mode of complex **(1)** and intercalation mode of complex **(2)**. The greater binding potential of complex **(2)** could be attributed to ring opening of the coordinated CBDCA in [Pd(byp)(CBDCA)] and creation of a very stable adduct stabilized by stacking interactions between the sugar group of DNA and both the bipyridine ring and the coordinated CBDCA ring as in the case of carboplatin [41]. The antitumor activity of the two complexes tested on some cancer cell lines as well as on one normal human melanocytes cell line reveals that the cytotoxicity of complex (**2)** was much higher than that of complex (**1)**, also interesting was the small impact of both complexes on the human normal cells, which may consider the two complexes as a specific target for DNA cancer cells.

Our results suggests that addition of glycine and CBDCA moiety to structure of Pd(II)-byp complex had improved the binding capacity and the antiproliferative properties of the anticancer ligands , and make [Pd(byp)(CBDCA)] a model for carboplatin with a prediction of better antitumor activity. There is a good agreement between spectroscopic, electrochemical studies and anti-cancer activity assays that could be correlated to further highlight the significance of this investigation.

Conflicts of interest

"There are no conflicts to declare".

FUNDINGS

We are deeply grateful for the financial support offered by King Abdullah Economic City (KAEC) (grant number AT35-374). Grant receiver is Haneen H. Al-Gedany.

REFERENCES:

1. Rosenberg B *mechanisms for the antitumor activity of platinum coordination complexes, cancer Chemother. Rep*. Part **(1)(59)** 589,(1975).
2. Pinto A L and Lippard S J Binding of the antitumor drug *cis* diamminedichloroplatinum(II) (cisplatin) to DNA, *Biochim Biophys. Acta*, 780, 167, (1985)
3. Divsalar A, Javad Bagheri M, Saboury A, Mansoori-Torshizi H, Amani M Investigation on the Interaction of Newly Designed Anticancer Pd(II) Complexes with Different Aliphatic Tails and Human Serum Albumin, *J. Phys. Chem*. B, **113,** 14035, (2009)
4. Li F H, Zhao G H, X H Wu, Synthesis, characterization and biological activity of lanthanum(III) complexes containing 2-methylene-1,10-phenanthroline units bridged by aliphatic diamines, *J. Inorg. Biochem.* 100, 36, (2006).
5. Neidle S, Ismail I M, Sadler P J ,The structure of the antitumor complex *cis*-(diammino) (1,1-clobutanedicarboxylato)-Pt(II): X ray and nmr studies, *J. Inorg. Biochem*. 13, 205,(1980).
6. Frey U, Ranford J D, Sadler P J, Ring-opening reactions of the anticancer drug carboplatin: NMR characterization of cis-[Pt(NH3)2(CBDCA-O)(5'-GMP-N7)] in solution. Inorg. Chem. 32, 1333 ,(1993)
7. Wilkinson R, Cox P J, Jones M, Harap K P, Selection of potential second generation platinum compounds, *Biochimie*, 60, 851(1978) .
8. Cleare N J, Hydes P C, Malerbi BW, Watkins D M, Anti-tumour platinum complexes : relationships between chemical properties and activity, Bichimie, 60, 835(1978).
9. Calvert A H et al ,Early clinical studies with *cis*-diammine-1,1-cyclobutane dicarboxylate platinum II, *Cancer Chemother. Pharmacol* 9, 140,(1982).
10. Evans B D, Raju K S, Calvert A H, Harland S J, Wiltshaw E, Phase II study of JM8, a new platinum

analog, in advanced ovarian carcinoma, *Cancer Treat. Rep* 67 997(1983)
11. Tinker N D, Sharma H L, Mc Auliffe C A In Platinum and other metal Coordination Compounds in Cancer Chemotherapy, M. Nicolini (Ed.), p. 144, Martinus Nijhoff Publ., Boston, MA (1988)
12. Canovese L, Cattalini L, Chessa G, Tobe M L, Kinetics of the Displacement of Cyclobutane-1 ,I - dicarboxylate from Diammine(cyc1obutane-1 ,I - dicarboxylato)platinum(11) in Aqueous Solution, *J. Chem. Soc., Dalton Trans*. **8,** 2135(1988).
13. Petrovic B , Bugarcic Z D, van Eldik R, Kinetic studies on the reactions of [Pd(dach)(X–Y)] complexes with some DNA constituents, *Dalton Trans.*, 6 807(2008).
14. Summa N, Soldatovic T, Dahlenburg L, Bugarcic Z D,. van Eldik R, The impact of different chelating leaving groups on the substitution kinetics of mononuclear PtII(1,2-trans-R,R-diaminocyclohexane)(X-Y) complexes**,** *J. Biol. Inorg. Chem*. 12, 461(2007).
15. Divsalar A, Saboury A A ,Yousefi R , Moosavi-Movahedi A A, Mansoori-Torshizi, Spectroscopic and cytotoxic studies of the novel designed palladium(II) complexes: beta-lactoglobulin and K562 as the targets, *International Journal of Biological Macromolecules* **40** 381(2007)
16. Shoukry A A DNA Binding and Equilibrium Investigation of the Interaction of a Model Pd(II) Complex with Some Selected Biorelevant Ligands**,** *J Solution Chem*. 43, 746 (2014).
17. Shoukry AA, Alghanmi R M Synthesis, DNA binding and complex formation reactions of 3-amino-5,6-dimethyl-1,2,4-triazine with Pd(II) and some selected biorelevant ligands, *Spectrochimica Acta Part A: Molecular and Biomolecular Spectroscopy* 138 , 932,(2015)
18. M. Feizi-Dehnayebi M, Dehghanian E, Mansouri-Torshizi H A novel palladium(II) antitumor agent: Synthesis, characterization, DFT perspective, CT-DNA and BSA interaction studies via in-vitro and in-silico approaches *Spectrochimica Acta Part A: Molecular and Biomolecular Spectroscopy* 249 , 119215,(2021)
19. Elgedany H H and Shoukry A A Synthesis, DNA binding and equilibrium investigation of Model Pd(II)pip complexes with some selected DNA unit-constituents**,** *International Journal of Basic & Applied Sciences* **18,** 6 (2018).
20. Pothing A , Casini A, Recent Developments of Supramolecular Metal-based Structures for Applications in Cancer Therapy and Imaging, 2019; *Theranostics* , 9(11): 3150–3169(2019)
21. Kumar Sharma N, Kumar Ameta R, Man Sing M Biological Impact of Pd (II) Complexes: Synthesis, SpectralCharacterization,In VitroAnticancer, CT-DNA Binding, and Antioxidant Activities, *International Journal of Medicinal Chemistry* 10,(2016)
22. Mansouri-Torshizi H , Zareian-Jahromi S, Ghahghaei A, Shahraki S, Khosravi F, and Heidari Majd M, Palladium(II) Complexes of Biorelevant Ligands. Synthesis, Structures, Cytotoxicity and Rich DNA/HSA Interaction Studies , *Journal of Biomolecular Structure and Dynamics (2017)*
23. Shoukry M M, Shoukry A A and Hafez M N Complex formation reactions between [Pd(piperazine)(H2O)2]2+ and biorelevant ligands: synthesis and equilibrium constants **.J.** *coord.Chem* **63,** 652 (2010).
24. Shoukry A A, Mohamed M S DNA-binding, spectroscopic and antimicrobial studies of palladium(II)complexes containing 2,2-bipyridine and 1-phenylpiperazine *Spectrochim. Acta Part A* **96,** 586(2012)
25. Raman N, Raja J D, Sakthivel A, Synthesis, spectral characterization of Schiff base transition metal complexes: DNA cleavage and antimicrobial activity studies *J. Chem. Sci.* **19** 303(2007).
26. Ishow E, Gourdon A, Launay J P, Observation of supramolecular p–p dimerization of a dinuclear ruthenium complex by 1H NMR and ESMS, *Chem. Commun*. 1909(1998).
27. Bates R G. Determination of pH: Theory and Practice, 2nd Edn, Wiley Interscience, New York(1975)
28. Gans P, Sabarini A, Vacca A An improved computer program for the computation of formation constants from potentiometric data.Inorg. Chim. Acta **18** 237(1976).
29. Pettit L SPECIES, available program supplied to the authors. Academic Software, Old Farm *Personal Communication*, University of Leeds (1993).
30. Abdel-Rahman L H, El-Khatib R M, Nassr L A E, Abu-Dief A, DNA binding ability mode, spectroscopic studies, hydrophobicity, and in vitro antibacterial evaluation of some new Fe(II) complexes bearing ONO donors amino acid Schiff bases, *Arabian Journal of Chemistry* **10** 1835(2017).
31. Shoukry A A, Complex formation reactions and equilibrium studies of mixed ligand complexes of diaqua (1-Phenyl piperazine)(Palladium)(II) with some biologically relevant ligands**,** *Int. J. Basic Appl. Sci*. 2 (1) 38(2013).
32. Shehata M R, Mixed ligand complexes of diaquo (2,2-bipyridine)palladium(II) with cyclobutane-1,1-dicarboxylic acid and DNA constituents, *Transition Metal Chemistry* **26,** 198(2001).
33. Sigel H, Massoud S S, Corfu N V Comparison of the extent of base back binding in complexes of divalent metal ions with guanine (GMP2-), inosine (IMP2-) and adenosine 5-monophosphate (AMP2-).The crucial role of N-7 basicity in metal ion-nucleic base recognition. *J. Am. Chem. Soc* **116** 2958(1994).
34. Hodgson D J, The stereochemistry of metal complexes of nucleic acid constituents**,** *Prog. Inorg. Chem.* **23,** 211(1977)
35. Marzilli L G, Metal-ion interactions with nucleic acids and nucleic acid derivatives, *Prog. Inorg. Chem.*,**23** 255 (1977)
36. Kumar R S, Arunachalam S DNA binding and antimicrobial studies of polymer-copper(II) complexes containing 1,10-phenanthroline and L-phenylalanine ligands. *Eur. J. Med. Chem.* 44, 1878(2009).
37. Kazem M A et al, A Pd(II) complex derived from pyridine-2-carbaldehyde oxime ligand: Synthesis, characterization, DNA and BSA interaction studies and in vitro anticancer activity, Journal of Molecular Structure 1219, 128479,**(2020)**

38. Kessissoglou D P, Synthesis, structure and interactions with DNA of novel tetranuclear,[Mn_4(II/II/II/IV)] mixed valence complexes *J. Inorg. Biochem*102, 618 (2008).
39. Mudasir E t, Wahyuni D H, Tjahjono N Y, Yoshioka, Inoue H, Spectroscopic studies on the thermodynamic and thermal denaturation of the ct-DNA binding of methylene blue, *Spectochim Acta, A* 77, 528 (2010).
40. Norden B, Tjerneld F., Binding of inert metal complexes to deoxyribonucleic acid detected by linear dichroism, *FEBS Lett*. 67, 368 (1976).
41. An Y, Liu S D, Deng S Y, Ji L N, Mao Z W, Cleavage of double-strand DNA by linear and triangular trinuclear copper complexes, *J. Inorg. Biochem* 100, 1586 (2006)
42. Shahabadi N and Mohammadi S, Synthesis Characterization and DNA Interaction Studies of a New Zn(II) Complex Containing Different Dinitrogen Aromatic Ligands**,** *Bioinorganic Chemistry and Applications*, 571913(2012) .
43. Kapicak L and Gabbay E J, Topography of nucleic acid helixes in solutions. XXXIII. Effect of aromatic cations on the tertiary structures of deoxyribonucleic acid *Journal of the American Chemical Society* 97(2) 403(1975).
44. Long E C and Barton J K, On demonstrating DNA intercalation *Accounts of Chemical Research* 23 271(1990).
45. Kaldor S W, Dressman B A, Hammond M et al., Isophthalic acid derivatives: amino acid surrogates for the inhibition of HIV-1 protease, *Bioorganic and Medicinal Chemistry Letters*, 5, **7** 721(1997) .
46. Hvastkovs E. G, Buttry D A, Characterization of Mismatched DNA Hybridization via a Redox-Active Diviologen Bound in the PNA−DNA Minor Groove *Langmuir*, **25(**6) 3839(2009).
47. Armistead P M, Thorp H H, Modification of indium tin oxide electrodes with nucleic acids: detection of attomole quantities of immobilized DNA by electrocatalysis *Anal. Chem.* **72,** 3764**(2009)**.
48. Welch T W and Thorp H H, Distribution of Metal Complexes Bound to DNA Determined by Normal Pulse Voltammetry *J. Phys. Chem.*, **100,** 13829**(1996)**.
49. Carter M T and Bard A J, Voltammetric studies of the interaction of tris(1,10- phenanthroline)cobalt(III) with DNA , *J. Am. Chem. Soc*., **109,** 7528(1987).
50. Hart J P, Electroanalysis of Biologically Important Compounds (Ellis Horwood Series in Analytical Chemistry), Ellis Horwood Ltd., England 1990.
51. Arjmand F, Aziz M, Tabassum S Cyclic Voltammetry-An Electrochemical Approach to Study Metal-based Potential Antitumor Drug-DNA Interaction *Curr. Anal. Chem.* **7,** 71(2011).